

International Journal of

INTELLIGENT SYSTEMS AND APPLICATIONS IN ENGINEERING

ISSN:2147-6799 www.ijisae.org Original Research Paper

Performance and Evolution of Glaucoma Detection in Retinal Fundus Images Using Various Deep Learning Architectures

¹Rajesh Kumar, ²Dr. Hare Ram Sah

Submitted:13/03/2024 **Revised**: 28/04/2024 **Accepted**: 05/05/2024

Abstract: The leading cause of irreversible eyesight loss worldwide is glaucoma. Early identification of glaucoma is difficult because symptoms don't appear until the disease is progressed. Routine glaucoma screening is recommended. The eye screening process now requires subjective assessments, which take time and energy. Ophthalmologists are few. Ophthalmologists use a two-step computerized glaucoma screening to reduce effort. This study analyzes advanced deep learning methods including ENet, ResNet50, GoogLeNet, inceptionv3, and AlexNet for glaucoma diagnosis. Glaucoma categorization and optic disc and cup segmentation are done using a pre-trained CNN. This approach calculates Cup-to-Disc Ratio more accurately. Compared to other designs, ENet is most accurate. Efficient Neural Networks (a subset of CNNs) optimize finite resources through lightweight and efficient inference. Training and testing the ENet architecture on a public Kaggle dataset yields 98.40% segmentation accuracy.

Keywords: ENet, ResNet50, GoogLeNet, inceptionv3, Optic Cup (OC) and Optic Disc (OD)

I INTRODUCTION

It is imperative for individuals with glaucoma to have an accurate diagnosis promptly in order to prevent additional harm and potential loss of vision. The World Health Organization (WHO) reports that 3.54 percent of persons aged 40 to 80 are affected with glaucoma. Individuals who are impacted may observe a deterioration in their visual acuity. The prevalence rate of the affected population is 12.5%, with individuals under the age of 40 exhibiting a higher probability of requiring healthcare compared to those aged 40 and above [1]. Elevated intraocular pressure is regarded as a causative element in the progression of glaucoma due to its harmful impact on the blood vessels and optic nerves within the eye. Glaucoma impacting the optic nerves can lead to complete blindness in both eyes or partial vision loss in one eye. Glaucoma often leads to irreversible blindness. If the condition impacts both eyes, then the likelihood of this happening is increased. Due to the subsequent events, this occurrence is commonly known as the "ophthalmic bandit". The condition of optic nerve dysfunction is sometimes referred to as a "silent disease" due to the absence of initial obvious symptoms. This is due to the fact that, during the initial phases of the illness, the majority of individuals do not display any symptoms all. Glaucoma is the leading cause of permanent visual impairment, second only to cataracts. Annually, glaucoma results in blindness for 12% of the population in the United States. According to a study [2], it is projected that by the year 2040, a total of 111.8

¹Ph.D. Scholar – Enrollment No. **21ENG7CSE0002,** Department of Computer Science and Engineering Institute of Engineering and Technology SAGE University, Indore (M.P.) India

E-mail – kumarpolyujn@gmail.com

²Professor – Department of Computer Science and Engineering Institute of Engineering and Technology SAGE University, Indore (M.P.) India

E-mail -- ramaayu@gmail.com

million people between the ages of 40 and 80 will be diagnosed with glaucoma worldwide. The prevalence of Alzheimer's disease in individuals aged 70 and above is 4.7%, which is higher than the 2.4% risk observed in the general population. When we use the term "retinal ganglion cell loss," or RGC, we are referring to a wide range of illnesses that cause the deterioration and eventual demise of RGCs. Insufficiency of ganglion cells in the retina can lead to problems with the neocortical nerve fiber layer and the optic nerve head (ONH), finally causing reduced visual acuity. Unmanaged glaucoma can lead to the deterioration of both central and peripheral vision. Due to the lack of a current pharmaceutical treatment or remedy for glaucoma, healthcare practitioners employ a combination of therapeutic and diagnostic methods to handle the problem. Without it, the development of equipment capable of autonomously detecting indications of eye problems would not be possible. The user's text is "[3]." Retinal fundus imaging is a technique that can be employed to examine and analyze the retina, macula, and vitreous. Additionally, it is possible to observe the present condition of the optic nerve. Ophthalmologists commonly employ a "fundus camera" to capture photographs of their patients' retinas. Retinal imaging can be used to detect the eye ailment known as glaucoma. Glaucoma ranks as the second most prevalent factor leading to blindness globally, following cataracts. Glaucoma alters the central optic nerve head (ONH) region. Examining these potential risk factors may assist in determining the presence of glaucoma. The optic nerve head transmits visual information to the brain upon receiving an image via the retina. By magnifying Figure 1, one may observe the retina in greater detail, revealing the presence of a fundus. An indication of the ocular condition known as glaucoma is the impairment of the optic nerves. Glaucoma is asymptomatic during its initial

stages, but it can eventually lead to blindness as it progresses. Timely diagnosis and treatment of glaucoma significantly improve the likelihood of preserving vision in the affected eye for patients. Excavating the optic cup alleviates pressure on the optic nerve at a precise stage of glaucoma. This statement provides a description of the optical disc and the optical cup. The term used to describe this is the "cup-to-disc ratio." The CDR value serves as a valuable tool for ophthalmologists to monitor the progression of glaucoma in their patients. To obtain CDR from a retinal image, a segmentation technique consisting of two steps is required. The CDR is acquired through the iterative application of the aforementioned technique.

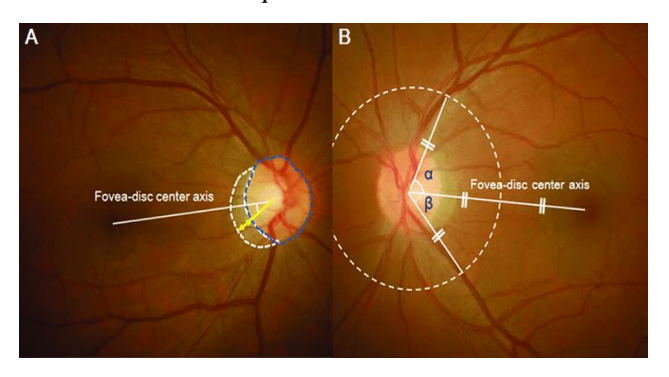


Fig 1: Glaucoma disease image

IV LITERARURE SURVEY

The disease known as glaucoma affects the nervous system and causes the death of ganglion cells. The maturation of the rim tissue and the compression of the optic nerve fiber both contribute to the development of a cup-shaped structure. Diagnosing structural damage and alterations in glaucoma is currently challenging due to significant limitations in disease detection techniques. In the absence of treatment, classic symptoms of glaucoma include visual field abnormalities, optic glaucomatous cupping, and intraocular pressure (IOP) higher than 22 mmHg. A degenerative eye illness known as glaucoma gradually weakens the optic disc. There are many difficult parts of diagnosing glaucoma, but one of the most difficult is finding cases where the patient does not show any symptoms. For patients, this means that the number of undiagnosed cases exceeds the number of diagnosed cases. Consideration of the optic cup disc's size and form is essential in the glaucoma diagnostic process. The characteristic of glaucomatous optic neuropathy is a longer upper portion of the cup than a shorter lower portion.

Nazmus Shakib et. al. 2022 [25] Glaucoma is a widely recognized leading cause of blindness and is among the most prevalent worldwide. Prompt identification and systematic examination are two vital components in the fight against this disease. The utilization of deep learning in this scenario seems promising. We conducted a performance evaluation of deep learning models using a dataset consisting of 1250 distinct pictures sourced from public databases. Clinicians commonly utilize fundus pictures in a clinical context to verify the existence of glaucoma. This article explores the present progress of the diagnostic framework in its journey towards achieving full deep learning capabilities. An assessment is conducted to evaluate and compare the efficacy of multiple deep learning frameworks.

YvesAttry, Kalin, et. al. 2022[42] The eye disease glaucoma is very serious and can damage your vision. An eye disease called optic neuritis can be very dangerous because it can damage nerves and cause sudden loss of vision. Several ideas have been combined with Machine Learning and Deep Learning models in an effort to find glaucoma. For a sickness that is so important, though, these models aren't good enough at making diagnoses. For this study, we've put together a bunch of different Deep Learning Architectures that meet different needs. A few of the models are MobileNetV2, DenseNet121, InceptionV3, Inception, ResNetV2, ResNet50, and VGG16. There are more people than just "G" and "NG" groups that these designs are meant to appeal to. In order to get the most accurate results, the information was preprocessed and put together from different sources. We used many different types of measures to rate our inventions, including recall, accuracy, F1-score, Cohen Kappa Score, and area under the curve (AUC).

VI PROPOSED METHOD

Failure to promptly identify and treat glaucoma, a complex illness that affects the optic nerve, can lead to permanent blindness or substantial visual impairment. Deep learning, a branch of machine learning, has demonstrated promising results in predicting the course and progression of glaucoma by utilizing several imaging and clinical data sets. Collect several images of the retinas from individuals with glaucoma and individuals without glaucoma. Ensure that the dataset includes a wide range of demographics and ethnicities. Ensure the authenticity and dependability of the data by implementing established imaging methodologies and quality assurance methods. Subsequently Before proceeding with the analysis, apply denoising, light normalization, and contrast enhancement techniques to the retinal images. To detect the regions of interest (ROIs) in the pre-processed retinal images, utilize an automated identification technique. The region of interest (ROI) refers to the specific area of a picture that encompasses the retina and optic disc. Utilize an automated segmentation technique to partition the ROI into segments that align with the optic disc and cup. Subsequent Perform segmentation on the optic disc and cup, and then utilize a pre-trained deep learning model (such as ResNet50, Enet, inceptionV3, Alexnet, or GoogleNet) on the segmented areas. This classifier utilizes the collected features to ascertain if a patient is afflicted

with glaucoma or not. Analyze the results of multiple classifiers and utilize the metrics obtained to ascertain the most optimal one.

Proposed Algorithm for Automatic Glaucoma Detection in Retinal Fundus Images

- 1. Select the retinal fundus image from dataset.
- Resize the image into desired pixels. 2.
- 3. Convert the input fundus RGB image into gray scale
- 4. Use Filtering to remove noise and blood vessels.
- Find maximum intensity pixel in the filtered image.
- Optic Disk region detection and smoothing & calculate optic disk radius.
- Optic Cup region detection and smoothing & calculate optic cup radius.
- Compute Cup to Disk ratio.
- If CDR is less than 0.3 then Normal Eye else Glaucoma affected Eye.
- 10. Using Deep Learning model like ResNet50, Enet, inceptionV3, Alexnet, GoogleNet for automatic Glaucoma detection.

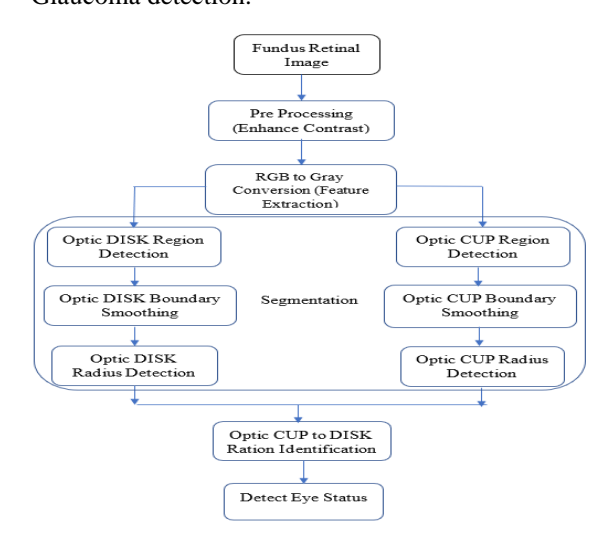


Fig 2: Flow Chart of Proposed Method

Data Collection-The dataset used for the deep learning platform consists of 1000 fundus images belonging to 39 classes.

https://www.kaggle.com/datasets/linchundan/fundusim age1000 All the Joint Shantou International Eye Center (JSIEC), which is in the city of Shantou in the province of Guangdong in China, gave us these 1,000 images of the back of the eye. There are 39 different types of pictures that make up the fundus. These pictures are just a small selection of the 209,494 fundus images that will be used to train, verify, and test our deep-learning platform.

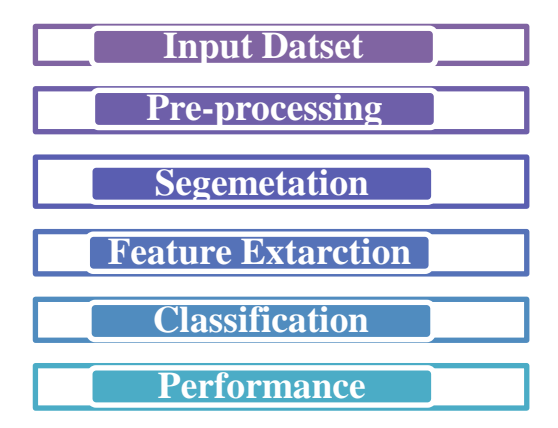


Fig 3: Deep Learning to overcome this defect

Pre-processing- Before applying any processing algorithm, it is essential to remove the noise from the input image. Most glaucoma detection approaches use a filter based on anisotropic diffusion. This technique is advantageous since it does not require any preliminary knowledge about the noise pattern or energy spectrum.

Pre-processing- The pre-processing processes commonly used to glaucoma photographs include:

Image transformation and scalability refer to the process of modifying and resizing images to meet specific requirements or to accommodate different display sizes and resolutions. Resizing glaucoma photos to a consistent size is crucial to provide uniformity across the collection, especially when the images have been collected at varying resolutions. Occasionally, it is necessary to crop an image in order to eliminate unwanted artifacts or emphasize a certain area of interest.

Differentiation Segmentation of the optic disc and cup is an essential and critical process in the identification and management of glaucoma. The optic disc, situated in the posterior region of the eye, serves as the point of entry and exit for the optic nerve. The cup, which is the central region of the disc, lacks nerve fibers. The cup-to-disc ratio is an essential parameter used to diagnose and stage glaucoma, as it provides valuable information about the extent of damage to the optic nerve. The presence of artifacts such as blood vessels, exudates, shadows, as well as the varying sizes, shapes, and appearances of the optic disc and cup make it challenging to separate them from retinal pictures.

Feature Extraction: After processing the input data, the next stage is feature extraction. This procedure entails extracting the relevant attributes from the input dataset in order to facilitate classification. The (GLCM) is a method used to characterize the textural properties of a picture. The subsequent procedures included in the computation of the GLCM are as follows:

- Select a certain distance, denoted as d, and an angle, denoted as θ, to determine the displacement between the pairs of pixels.
- ❖ For every pixel (x,y) in the picture, calculate the grey-level value i at (x,y) and the grey-level value j at (x+dcos(\theta), y+dsin(\theta)), where d represents the selected distance and \theta represents the selected angle.
- ❖ Increment the respective entry in the GLCM matrix G(i,j) by 1. Put simply, if the pixel pair (i,j) appears at displacement d and angle \theta, then G(i,j) is increased by 1.
- Repeat steps 2-3 for every pixel in the picture.
- ❖ Normalize the GLCM matrix by performing element-wise division with the total number of pixel pairs corresponding to the specified displacement and angle.

V DEEP LEARNING ARCHITECTURE

Scientists have developed deep learning algorithms that aim to replicate the structure and functions of the human brain. These algorithms let computers learn from large datasets and make accurate conclusions or predictions.

Resnet50- ResNet50 is a convolutional neural network architecture composed of 50 layers. The ResNet50 model may be defined as follows:

ResNet50 first use a convolutional layer to extract features from the input image I. Let us represent the result of this layer as F1, which can be formulated as:

$$F1 = conv1(I)$$
 Eq.1

The term "conv1" denotes the convolutional layer. Following the first convolutional layer, ResNet50 employs many residual blocks, each including several convolutional layers.

$$y_i = x_i + F_i(x_i)$$
 Eq.2

the output of the block is denoted as y_i. The inclusion of residual connections in each block enables the model to learn residual functions that are more amenable to optimization. Let us represent the result of this layer as F2, which can be mathematically represented as:

$$F2 = avg_pool(y_n)$$
 Eq.3

Let us represent the result of this layer as y, which can be formally defined as:

$$y = fc(F2)$$
 Eq.4

Where fc denotes the fully connected layer.

Overall, the ResNet50 model can be represented mathematically as a function:

$$y = fc(avg_pool(residual_blocks(conv1(I))))$$

Eq.5

Where I represent the input image, conv1 represents the

initial convolutional layer, residual_blocks represents the set of residual blocks, avg_pool represents the global average pooling layer.

AlexNet- In its mathematical expression, starting with an input image I, the initial layer is a convolutional layer applying filters to extract local features, generating a set of feature maps denoted as F_1.Mathematically, we can write this operation as:

$$F_1 = Conv(I, W_1) + b_1$$
 Eq.6

Where Conv is the convolutional operation, W_1 represents the set of filters, and b_1 represents the bias terms for each filter. The next layer is a by taking the maximum value in each local region. This is represent by:

$$F_2 = MaxPool(F_1)$$
 Eq.7

The last two layers consist of convolutional layers, labeled as F_3 and F_4, followed by an additional max pooling layer to further reduce the size of the feature maps. Following the convolutional layers, there are three completely linked layers, specifically referred to as F_5, F_6, and F_7. These layers use the feature maps from the preceding layer to calculate a conclusive output vector. From a mathematical perspective, we may express this as:

$$y = Softmax (F_8)$$
 Eq.8

Let y be the projected output vector. In summary, the AlexNet model may be mathematically expressed as a function:

$$y = f(I) Eq. 10$$

Let y denote the expected output, I represent the input picture, and f is the function that calculates the output.

ENet-ENet, Developed specifically for the explicit objective of doing real-time semantic image segmentation.

The architecture of ENet consists of several layers, including convolutional, max pooling, batch normalization, and bottleneck layers. The mathematical representation of ENet can be expressed by equation (f). The function accepts an input image I and outputs a set of segmented pixels M. An approach to partition the components of the function f is as follows:

$$M = f(I) = L_n(L_{n-1}(...(L_2(L_1(I)))))$$
 Eq.11

where the letter L_i represents the i-th layer of the global network.

The initial layer of ENet is comprised of convolutional layers, which are employed for the purpose of extracting information from the input image. The next step is to limit the number of channels in the feature maps by employing a series of bottleneck layers. This is done in order to lessen the amount of computational effort that is being

done on the network. According to the following mathematical expression, the bottleneck layer can be stated as follows:

$$y = L_{\text{bottleneck}}(x) = \text{relu(conv}_1x1(x) * \text{relu(conv}_3x3(\text{conv}_1x1(x))$$
 Eq.12

the input feature map is denoted by x, the convolutional layers conv 1x1 and conv 3x3 have kernel sizes of 1x1 and 3x3, respectively, and the symbol * describes element-wise multiplication. In addition, Net makes use of a layer that is referred to as a "split-and-merge" layer. This layer divides the feature maps into smaller pieces, performs various operations to each of those portions, and then combines them back together. This helps to lower the amount of processing resources that are required by the network while yet preserving its capacity to record finegrained features. One of the outputs of the last layer of ENet is a collection of segmented pixels, which may be mathematically expressed as follows:

 $softmax(conv_{final}(L_{drop}(L_{global}(L_{last}(L_{max})))))$ $\{sum\}(L_{concat})(x)$

Eq.13

where conv {final} is a convolutional layer that produces the final output, L_{drop} is a dropout layer to prevent overfitting, L_{global} is a global average pooling layer, L_{last} is a final convolutional layer, L_{sum} is a layer that sums the feature maps from different stages of the network,

InceptionV3- Image identification tasks are often performed with the help of the deep learning model known as InceptionV3. It is possible to provide a description of the mathematical equation for the InceptionV3 model as

InceptionV3 begins the process of extracting features from an input picture I by first applying a convolutional layer. The output of this layer is a collection of feature which are represented by the symbol F_0.Following this, the feature maps F_0 are introduced into a sequence of "inception modules," each of which is comprised of several parallel convolutional layers with varying filter sizes. It is possible for the model to better capture the structure of the input picture thanks to these convolutional layers, which are intended to collect information at varying sizes and resolutions. In order to distinguish the output of the i-th inception module, we will refer to it as F_i. The following is a methodology that may be used to calculate the output of the whole InceptionV3 model:

$$y = f(I) = g(h(F_n))$$
 Eq. 14

In this equation, y stands for the outcome that is predicted, I stands for the image that is input, and f is the function

that computes the output based on the input. Both g and h are functions that are defined by the InceptionV3 model in the following manner:

g = global_average_pooling_2d(F_n) Eq.15

h = dense(g)

Through the use of the global_average_pooling_2d operation, the InceptionV3 model may be mathematically represented as a function. This operation is responsible for calculating the average of each feature map over its physical dimensions. A dense layer, which is a completely linked layer that is responsible for creating the final output of the model, is then fed the result of this operation once it has been processed.

$$y = f(I) = g(h(F_n))$$
 Eq.16

The variables in this context are defined as follows: I represents the input picture, y represents the expected outcome, and F_n represents the result of the model's final inception module. Multiple levels are accountable for executing the function f. The layers include of convolutional layers, inception modules, a fully linked layer, and a global average pooling section.

GoogleNet - GoogleNet, sometimes referred to as Inception v1, is a sophisticated deep learning model designed specifically for the purpose of image identification tasks. The mathematical representation of GoogleNet may be expressed as a function:

$$y = f(I) Eq.17$$

Let y denote the expected output, I represent the input picture, and f is the function that calculates the output based on the input. The implementation of this function involves a sequence of layers, each of which carries out a distinct action on the input.

The architecture of GoogleNet may be delineated as follows:

Fully connected layers: The ultimate result of a model is produced by the completely linked layers, which receive the output from the previous layer. The mathematical formulation of the Inception module may be stated as follows:

$$y = [C1, C2, C3, C4]$$
 Eq.18

The outputs of four parallel convolutional layers with various filter widths are represented by C1, C2, C3, and C4, and the concatenation of these outputs is denoted by brackets. The Inception module produces a collection of feature maps that effectively capture features at various sizes.

The mathematical representation of GoogleNet may be expressed as:

y = W5(W4(W3(W2(W1(I)Eq.19 In the given context, I am denoted as the input picture. W1 to W5 are used to symbolize the weights of the five layers in the model. Lastly, y represents the ultimate output of the model. The user's text is "[21-22]".

VII RESULTS AND DISCUSSION

Preprocessing methods like as contrast enhancement, noise reduction, and picture normalization may be used on retinal images. Contrast enhancement is a technique that may be used to amplify the differences between various areas of a picture, facilitating the differentiation between healthy and sick parts. Noise reduction methods may be used to eliminate any abnormalities or irregularities in the picture that might impede the identification of diseaserelated characteristics. Image normalization methods may be used to normalize the pictures by addressing variances in lighting and image size. This can enhance the accuracy and dependability of the feature extraction process. Following the preprocessing stage, feature extraction is conducted to discern pertinent data from the retinal pictures. Multiple characteristics may be derived, including texture, color, form, and size-related attributes. Subsequently, these characteristics are inputted into a feature selection process, whereby pertinent and significant characteristics are recognized and chosen for categorization.

The training of these algorithms involves utilizing a labeled dataset of retinal images, where different classes signify whether glaucoma is present or absent. Once trained, the classification algorithm can be applied to new, unlabeled retinal images to predict the presence or absence of glaucoma.

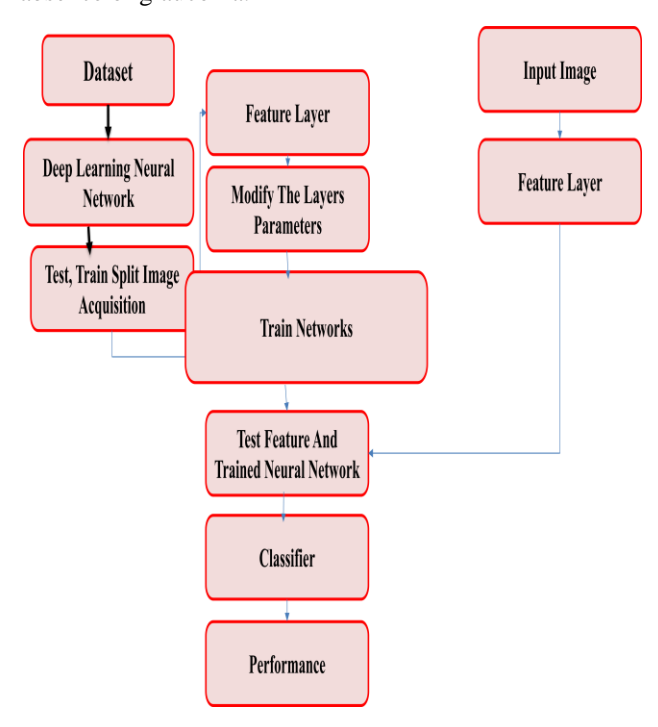


Fig 4: Deep learning to overcome this defect

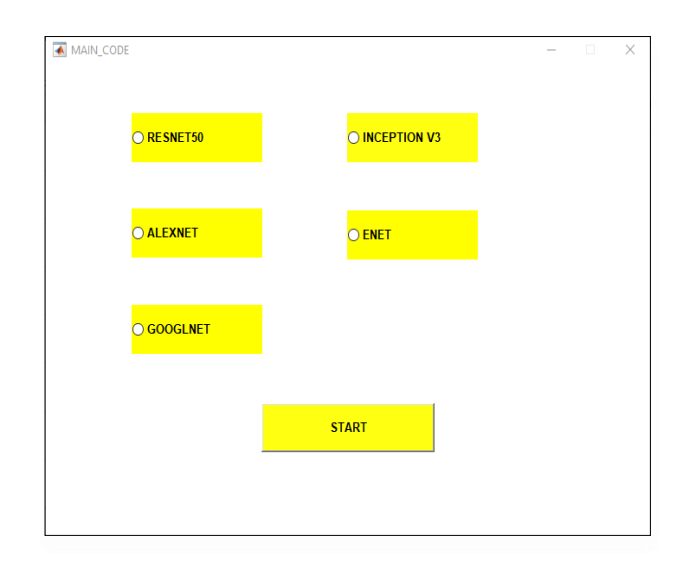


Fig 5: GUI windows of deep learning models

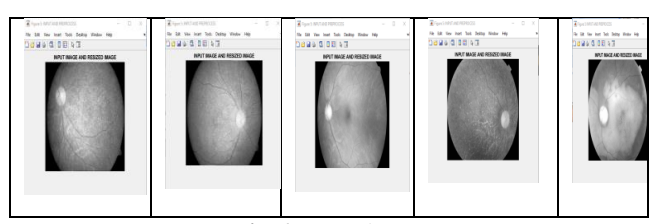


Fig 6: Input images

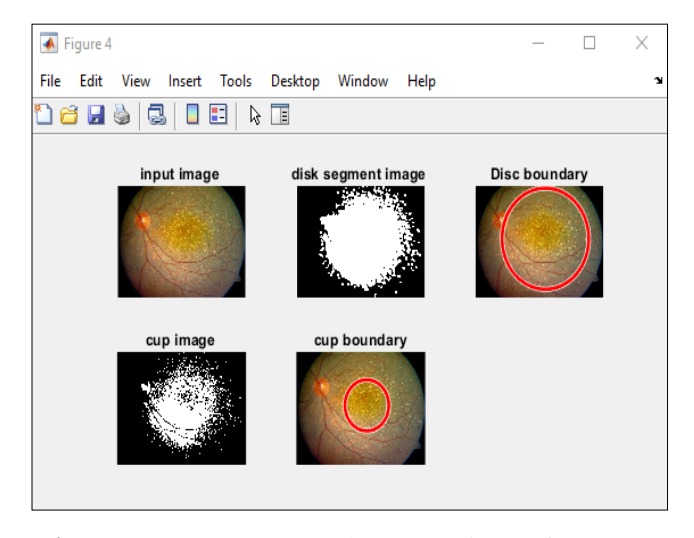


Fig 7: Image pre-process and segmentation performance

The diagnosis of glaucoma depends on determining the size and morphology of the optic disc. As previously stated, the typical size of an optic disc in a healthy individual is 1.2-2.5 mm in diameter and has a vertically oval form.

Regarding the precise measurements of an optic disc, there is much debate among scholars. A disk with a diameter of 1.8 mm or more is classified as gigantic, whereas a disc with a diameter of 1.2 mm or less is classified as little. Although the majority of research

employ comparable cutoff values, there could be slight variations.

When the size of the optic disc is too large, the optic cup will also be excessively large, hence complicating the analysis of the cup-to-disc ratio (CDR). The CDR is an essential diagnostic tool for glaucoma. The size of the optic disc can also impact the results of the visual field test and other diagnostic procedures. Glaucoma diagnosis and management depend on precise measurements and documenting of the size and structure of the optic disc. The margin of the optic nerve head (ONH), also known as the optic disc rim, refers to the outer edge of the ONH in clinical contexts. The optic disc is a rounded or oval area on the retina where the axons of retinal ganglion cells (RGCs) come together to create the optic nerve. It is considered a part of the anatomical structure known as the optic nerve head (ONH). Optic nerve injury may indicate the onset of glaucoma, hence assessing the health and look of the optic disc margin might provide valuable diagnostic information for evaluating the condition. Clinicians employ a range of technologies, such as fundus photography, ophthalmoscopy, and optical coherence tomography (OCT), to assess the edge of the optic disc.

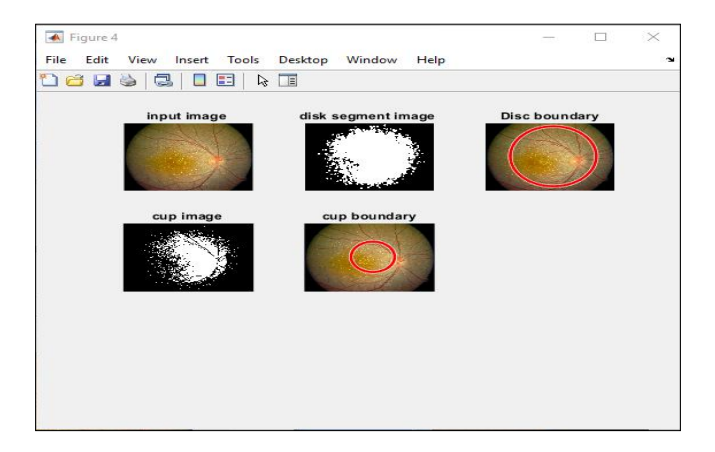


Fig 8: Image pre-process and segmentation performance of inception v3

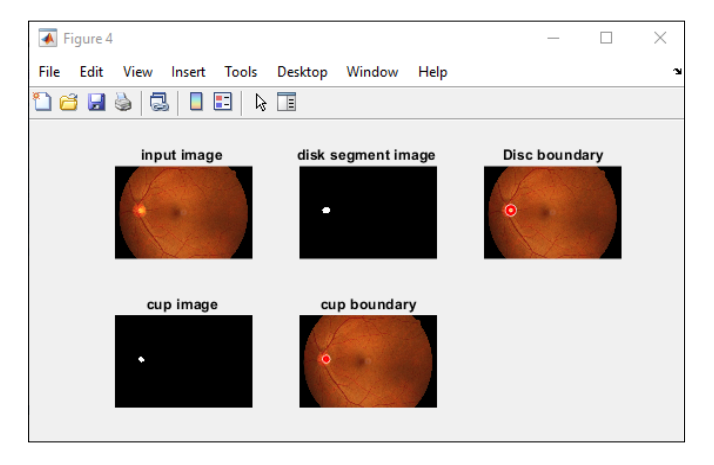


Fig 9: Image pre-process and segmentation performance of AlexNet

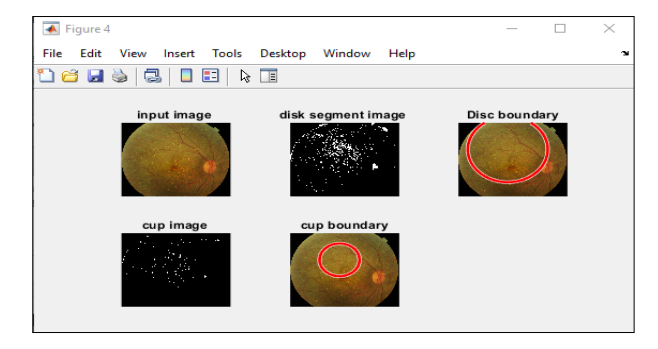


Fig 10: Image pre-process and The efficacy of ENet's segmentation system

The efficacy of ENet's segmentation system

The optic nerve plays a crucial role in vision by transmitting electrical impulses that convey visual information from the eye to the brain. The brain utilizes this information to create images. The Cup-to-Disc Ratio (CDR) is a crucial measurement used to diagnose glaucoma, a progressive eye disease that can cause permanent vision loss. Before attempting to forecast the possibility of cup-to-disc ratio (CDR), it is necessary to compare the size of the optic cup, which is the center depression of the disc, with the size of the disc itself. Individuals with glaucoma are at an elevated risk of developing optic nerve fibrosis, resulting in an enlargement of the optic cup relative to the optic disc. In order to diagnose glaucoma, it is important to have an optic cup size that exceeds the size of the optic disc. Figure 12 depicts the pertinent locations that need to be taken into account while calculating the CDR ratio.

The convergence of nerve fibers to form the optic nerve occurs in the region of the retina called the optic cup, which is highly illuminated. Conversely, the optic disc area offers a more precise indication of the brightest point contained inside the broader optic disc region.

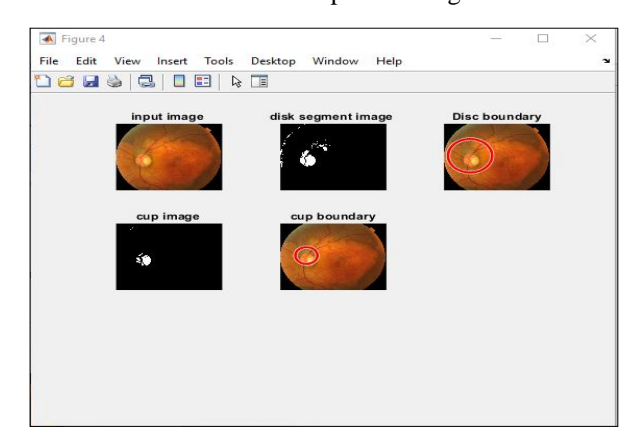


Fig 11: Image pre-process and segmentation performance of GoogLeNet

Table 1 Performance comparison of CDR and RDR

Deep learning models	CDR	RDR
ENet	0.55	0.41
InceptionV3	0.53	0.44
AlexNet	0.63	0.29
ResNet	0.179	2.45
Google net	0.44	0.65

Table 1: showing with the performance metrics of various deep learning models for glaucoma diagnosis.

The rim-to-disc ratio (RDR) and cup-to-disc ratio (CDR) are popular glaucoma diagnostic tools.

The study predicted CDR and RDR from retinal pictures using five deep learning models: ENet, InceptionV3, AlexNet, ResNet, and GoogleNet. The table shows results. The table shows model accuracy and error rate for each ratio.

AlexNet had the highest CDR prediction accuracy of 0.63, while ResNet had the lowest at 0.179. ResNet outperformed AlexNet in RDR prediction with 2.45 accuracy. AlexNet performed poorly with 0.29 accuracy. InceptionV3 and GoogleNet performed similarly in both ratios, while ENet excelled in CDR but failed in RDR.

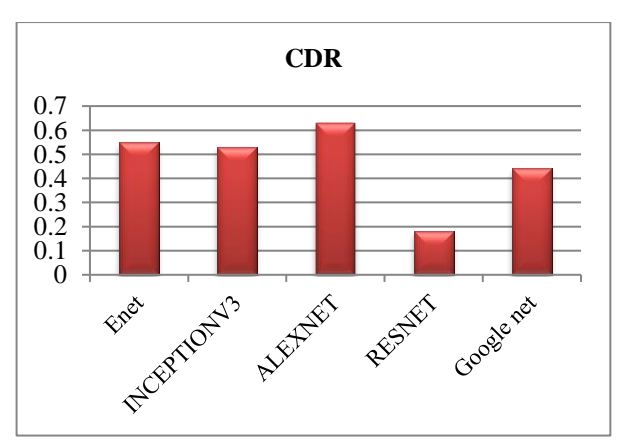


Fig 12: Performance comparison of CDR for different architecture

CDR is an important biomarker used in glaucoma detection because it can help to recognize individuals who are at superior risk for developing the disease or who may already have early signs of the disease. In addition to CDR, other important biomarkers for glaucoma include intraocular pressure (IOP), visual field testing, and nerve fiber layer thickness measurement. Automated systems that use image analysis techniques can be used to accurately measure the CDR from fundus photographs, which can aid in the early detection and management of glaucoma. These systems can help to improve the

efficiency and accuracy of glaucoma screening programs, which are critical for preventing vision loss and blindness in individuals with the disease.

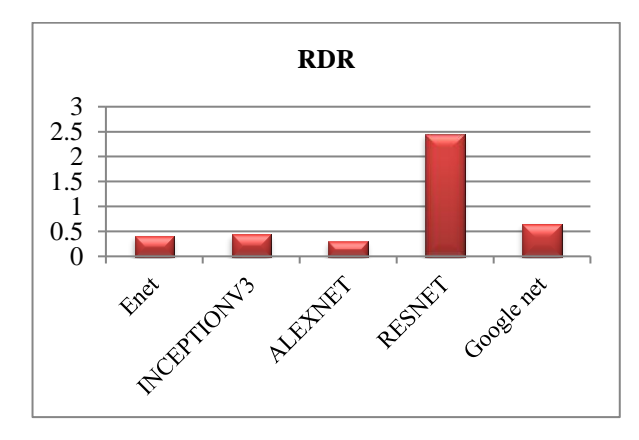


Fig 13: Performance comparison of RDR for different architecture

The average CDR (cup-to-disc ratio) is 0.4, which means that the size of the optic cup (the central depression within the optic disc) is 40% of the size of the optic disc. However, normal CDR ratios can vary from 0.0 to 0.9 due to inter-individual differences in disc and cup size. In normal individuals, CDR ratios typically range from less than 0.3 (seen in 66% of normal individuals) to greater than 0.5 (seen in only 6-10% of normal individuals).

Table 2 Performance comparison of different deep learning architecture

Deep Learning Models	Accuracy(%)	Sensitivity (%)	Specificity (%)
Enet	97.88	97.52	94.53
InceptionV3	97.57	83.57	86.57
AlexNet	94.50	83.50	86.50
ResNet	91.31	86.31	84.31
GoogLeNet	97.53	87.53	81.53

Table 2: giving a summary of the characteristics and performance indicators of various deep-learning glaucoma detection models. Often used to assess how well binary classification models are performing, the metrics that are offered include specificity, sensitivity, and accuracy. According to the table, ENet had the best performance in identifying glaucoma, with a sensitivity of 97.52%, specificity of 94.53%, and accuracy of 97.88%. InceptionV3 and GoogLeNet demonstrated higher accuracy (97.57% and 97.53%, respectively) in comparison to ENet; nevertheless, their sensitivity and specificity were lower.

Comparable to ENet in terms of sensitivity and specificity, AlexNet has a lower accuracy rate of 94.50%. ResNet displayed less sensitivity and the lowest accuracy rate (91.31%) of all the tested models.

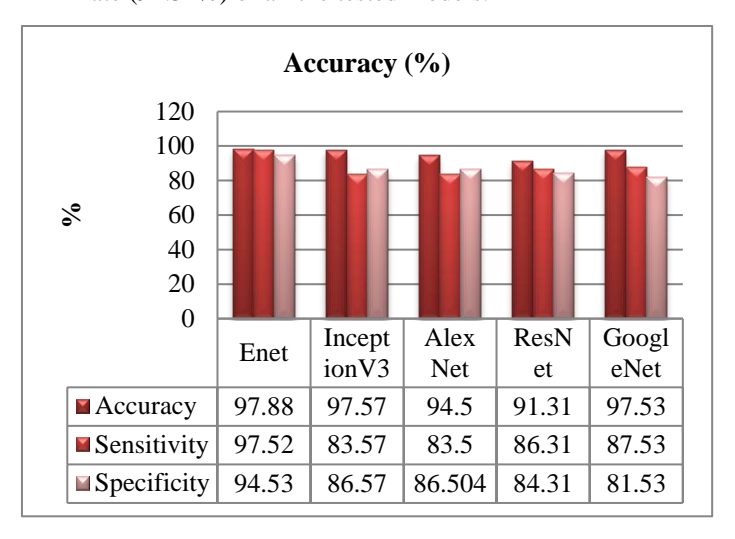


Fig 14: Performance comparison of different deep learning architecture

Table 3 Segmentation performance of the dissimilar deep learning models

Deep Learning Models	Jaccard Coefficient (%)	Dice (%)	Classification Error (%)
Enet	95.21	94.57	2.42
InceptionV3	94.63	86.21	2.49
AlexNet	94.32	87.32	2.64
ResNet	94.70	91.36	2.68
GoogleNet	93.52	92.52	2.46

Table 3: showing with the performance metrics of different deep learning models for a specific task, possibly related to medical image segmentation. The metrics reported are the Jaccard coefficient, Dice coefficient, and classification error, which are frequently used to calculate approximately the performance of segmentation models.

According to the table, ENet had the highest Jaccard coefficient and Dice coefficient, indicating the best performance for the task with scores of 95.21% and 94.57%, respectively. The other models had lower but still competitive scores, with ResNet having the second-highest Jaccard and Dice coefficients of 94.70% and 91.36%, respectively. InceptionV3, AlexNet, and GoogLeNet had slightly lower scores; but were still relatively close in performance to ENet and ResNet.

Regarding the classification error, all models had low error rates ranging from 2.42% to 2.68%, indicating high accuracy for the performance

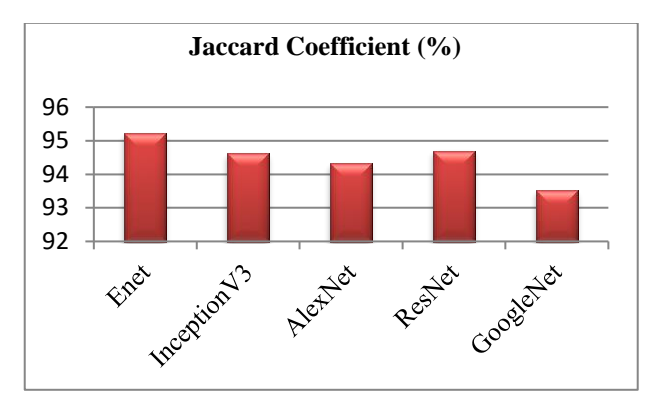


Fig 15: Jaccard Coefficient (%) performance of the different deep learning models

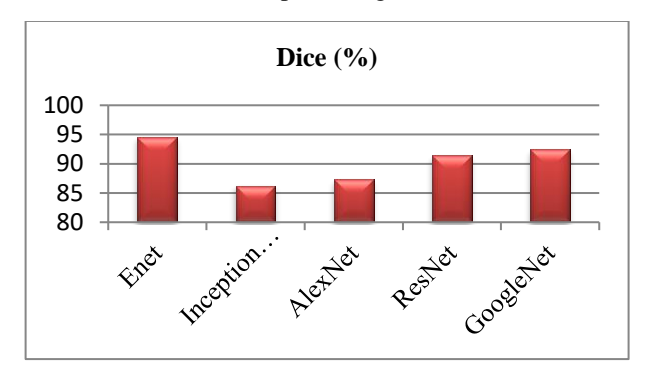


Fig 16: Dice performance of the different deep learning models

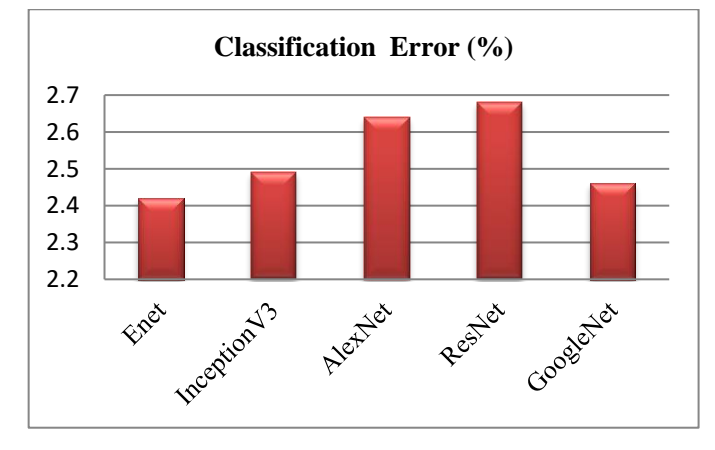


Fig 17: Classification Error (%) of the different deep learning models

VIII CONCLUSION

This research discovered that fundus photos have the capacity to identify glaucoma in both its advanced and early stages using deep learning algorithms. The models were assessed using various deep learning architectures, including InceptionV3, GoogLeNet, AlexNet, ENet, and ResNet. These designs were applied to a dataset gathered from a previous study. Due to the scarcity of pictures in the Fundus dataset, transfer learning was employed. ENet outperformed the other models in accurately diagnosing cases of both early and advanced glaucoma, as evidenced by its superior accuracy, specificity, and area under the ROC curve. ENet demonstrated improved performance in terms of sensitivity and area under the ROC curve

specifically for the classification of advanced glaucoma, despite this being the case. The sensitivity and specificity values of a diagnostic test are occasionally debated. The researchers concluded that the ENet model outperformed the other models in accurately diagnosing both advanced and early stages of glaucoma.

Acknowledgements

I would want to express my gratefulness and acknowledgement to my supervisor, Dr. Hare Ram Sah, without whom I would not have been able to do this task. The direction and suggestions that he provided helped me through each and every step of the process of producing my research paper. In addition, I would want to take this opportunity to convey my appreciation to the members of my committee for giving me the opportunity to have a positive experience during my defense and for the insightful comments and recommendations that you gave.

In addition, I would like to extend my heartfelt gratitude to my Niece (Sister's Daughter), Dr. Aahana Kumar as, for her unwavering support and understanding throughout the process of doing my research and completing my thesis.

There was no department that provided funding for this activity. It is self-funded.

Author Contributions

Rajesh Kumar:

Conceptualization, Methodology, Software, Field study, Data curation, Writing-Original draft preparation, Software, Validation, Field study.

Dr. Hare Ram Sah:

Visualization, Investigation, Writing Reviewing and Editing.

Conflicts of interest

Regarding the publishing of this research, the authors affirm that they do not have any competing interests or conflicts of interest.

Reference

- [1] Agarwal, S. Gulia, S. Chaudhary, M. K. Dutta, R. Burget, K. Riha, Automatic glaucoma detection using adaptive threshold based technique in fundus image, in *(TSP.)*, IEEE, 2015, 416–420.
- [2] Bibiloni, M. M. S. Missen, A. Rashid, Diabetic retinopathy techniques in retinal images: A review, *Artif. Intell. Med.*, **97** (2019), 168–188.
- [3] Bokhari, T. Syedia, M. Sharif, M. Yasmin, S. L. Fernandes, Fundus image segmentation and feature extraction for the detection of glaucoma: A new approach, *Curr. Med. Imaging Rev.*, 14 (2018), 77–87.

- [4] Christoph Haarburger; Jörg-Christian Kirr Marcel Menke Jakob Nikolas Kather; Johannes Stegmaier; Christiane Kuhl; Sven Nebelung; Daniel Truhnlevating Fundoscopic Evaluation to Expert Level Automatic Glaucoma Detection Using Data from the Airogs Challenge 2022 IEEE International Symposium on Biomedical Imaging Challenges (ISBIC) Year: 2022 | Conference Paper | Publisher: IEEE
- [5] Costagliola, R. Dell'Omo, M. R. Romano, M. Rinaldi, L. Zeppa, F. Parmeggiani, Pharmacotherapy of intraocular pressure: part i. parasympathomimetic, sympathomimetic and sympa-tholytics, *Expert Opin. Pharmacother.*, 10 (2009), 2663–2677.
- [6] Da-Wen Lu; Wei-Wen Hsu; Yu-Chuan Huang; Lung-Chi Lee; Jing-Ming Guo; Yu-Ting Hsiao; I-Hung Lin; Yao-Chung Chang; Mei-Lan Ko Visual Interpretability of Deep Learning Models in Glaucoma Detection Using Color Fundus Images 2022 IET International Conference on Engineering Technologies and Applications (IET-ICETA) Year: 2022 Conference Paper | Publisher: IEEE
- [7] Deo Paolo R. Danao; Daniel Martin N. Mababangloob; Jennifer C. Dela Cruz Machine Learning-based Glaucoma Detection through Frontal Eye Features Analysis 2022 IEEE 13th Control and System Graduate Research Colloquium (ICSGRC) Year: 2022 | Conference Paper | Publisher: IEEE
- [8] Dina ZatusivaHaq;'LabbaAwwabi; ShintamiChusnulHidayati; DarlisHerumurti Glaucoma Detection Based-on Convolution Neural Network and Fundus Image Enhancement 2022 10th International Conference on Information and Communication Technology (ICoICT)Year: 2022 | Conference Paper | Publisher: IEEE
- [9] Duy Doan; Phuong Thanh Tai Ho; Thanh Thien Nguyen; Thanh Nhan Ngo; Thi Thuy Tien Pham; Minh Son Nguyen Implementation of Complete Glaucoma Diagnostic System Using Machine Learning and Retinal Fundus Image Processing 2022 International Conference on Advanced Computing and Analytics (ACOMPA) Year: 2022
- [10] Fengze Wu; Marion Chiariglione; Xiaoyi Raymond Gao Automated Optic Disc and Cup Segmentation for Glaucoma Detection from Fundus Images Using the Detectron2's Mask R-CNN 2022 International Symposium on Multidisciplinary Studies and Innovative Technologies (ISMSIT) Year: 2022 | Conference Paper | Publisher: IEEE
- [11] Gupta, M. Tiwari, S. S. Lamba, Visibility improvement and mass segmentation of mammogram images using quantile separated histogram equalization with local contrast enhancement, *CAAI Trans. Intell. Technol.*, **4** (2019), 73–79.

- [12] H. A. Quigley, A. T. Broman, The number of people with glaucoma worldwide in 2010 and 2020, *Br. J. Ophthalmol.*, **90** (2006), 262–267.
- [13] H. A. Quigley, Neuronal death in glaucoma, *Prog. Retin. Eye Res.*, **18** (1999), 39–57.
- [14] J. Shingleton, L. S. Gamell, M. W. O'Donoghue, S. L. Baylus, R. King, Long-term changes in intraocular pressure after clear corneal phacoemulsification: Normal patients versus glaucoma suspect and glaucoma patients, *J. Cataract. Refract. Surg.*, 25 (1999), 885–890.
- [15] Juan S. Carrillo; Jorge Villamizar; Giovanni Calderón; Juan Rueda; Lola Bautista; Jose E. Castillo Glaucoma Detection using Fundus Images with Mimetic Anisotropic Filtering and Convolutional Neural Networks 2022 E-Health and Bioengineering Conference (EHB) Year: 2022 | Conference Paper | Publisher: IEEE
- [16] K. F. Jamous, M. Kalloniatis, M. P. Hennessy, A. Agar, A. Hayen, B. Zangerl, Clinical model assisting with the collaborative care of glaucoma patients and suspects, *Clin. Exp. Ophthalmol.*, 43 (2015), 308–319.
- [17] Latif, A. Rasheed, U. Sajid, J. Ahmed, N. Ali, N. I. Ratyal, et al., Content-based image retrieval and feature extraction: a comprehensive review, *Math. Probl. Eng.*, 2019.
- [18] Lei Yang; Yao Xie; Md Rafiqul Islam; Guandong Xu Big Data and Artificial Intelligence (AI) to Detect Glaucoma 2022 9th International Conference on Behavioural and Social Computing (BESC) Year: 2022 | Conference Paper | Publisher: IEEE
- [19] Lim Willoughby, D. Ponzin, S. Ferrari, A. Lobo, K. Landau, Y. Omidi, Anatomy and physiology of the human eye: effects of mucopolysaccharidoses disease on structure and function—a review, *Clin. Exp. Ophthalmol.*, **38** (2010), 2–11.
- [20] M. R. K. Mookiah, U. R. Acharya, C. M. Lim, A. Petznick, J. S. Suri, Data mining technique for automated diagnosis of glaucoma using higher order spectra and wavelet energy features, *Knowl. Based. Syst.*, 33 (2012), 73–82.
- [21] M. R. K. Mookiah, U. R. Acharya, C. M. Lim, A. Petznick, J. S. Suri, Data mining technique for automated diagnosis of glaucoma using higher order spectra and wavelet energy features, *Knowl. Based. Syst.*, **33** (2012), 73–82.
- [22] M. R. K. Mookiah, U. R. Acharya, C. M. Lim, A. Petznick, J. S. Suri, Data mining technique for automated diagnosis of glaucoma using higher order spectra and wavelet energy features, *Knowl. Based. Syst.*, **33** (2012), 73–82.
- [23] M. ShanmugaEswari; S. Balamurali A Pragmatic Glaucoma Detection Based On Deep Neural Network Strategy 2022 First International

- Conference on Electrical, Electronics, Information and Communication Technologies (ICEEICT) Year: 2022 | Conference Paper | Publisher: IEEE
- [24] Maninis, M. U. Akram, K. Wazir, S. M. Anwar, M. Majid, Autonomous glaucoma detection from fundus image using cup to disc ratio and hybrid features, in *ISSPIT*.), IEEE, 2015, 370–374
- [25] Nazmus Shakib Shadin; Silvia Sanjana; Sovon Chakraborty; Nusrat Sharmin Performance Analysis of Glaucoma Detection Using Deep Learning Models2022 International Conference on Innovations in Science, Engineering and Technology (ICISET) Year: 2022 | Conference Paper | Publisher: IEEE
- [26] Nazmus Shakib Shadin; Silvia Sanjana; Sovon Chakraborty; Nusrat Sharmin 2022 Performance Analysis of Glaucoma Detection Using Deep Learning Models 2022 International Conference on Innovations in Science, Engineering, and Technology (ICISET) , 2022, IEEE
- [27] P.S. Nandhini; P. Srinath; P. Veeramanikandan Detection of Glaucoma using Convolutional Neural Network (CNN) with Super Resolution Generative Adversarial Network (SRGAN) 2022 3rd International Conference on Smart Electronics and Communication (ICOSEC) Year: 2022 | Conference Paper | Publisher: IEEE
- [28] Parag Jibhakate; ShreshthaGole; Prachi Yeskar; Neeraj Rangwani; Aishwarya Vyas; Kanchan Dhote Early Glaucoma Detection Using Machine Learning Algorithms of VGG-16 and Resnet-50 2022 IEEE Region 10 Symposium (TENSYMP) Year: 2022 | Conference Paper | Publisher: IEEE
- [29] RajaL. Han, J. Van Hemert, B. Li, Automatic extraction of retinal features from colour retinal images for glaucoma diagnosis: a review, *Comput. Med. Imaging Graph.*, **37** (2013), 581–596.
- [30] Riley Kiefer; Jessica Steen; Muhammad Abid; Mahsa R. Ardali; Ehsan Amjadian A Survey of Glaucoma Detection Algorithms using Fundus and OCT Images 2022 IEEE 13th Annual Information Technology, Electronics and Mobile Communication Conference (IEMCON) Year: 2022 | Conference Paper | Publisher: IEEE
- [31] Riya N. Naik; Prajyot P. Naik; Sharanya R. Shirali; Richa R. Gaunker; PratikshaShetgaonkar; Shailendra Aswale Retinal Glaucoma Detection: An Overview 2022 3rd International Conference on Intelligent Engineering and Management (ICIEM) Year: 2022
- [32] S. Maheshwari, V. Kanhangad, R. B. Pachori, S. V. Bhandary, U. R. Acharya, Automated glaucoma diagnosis using bit-plane slicing and local binary pattern techniques, *Comput. Biol. Med.*, **105** (2019), 72–80.

- [33] Sarhan, J. Rokne, R. Alhajj, Glaucoma detection using image processing techniques: A literature review, Comput. Med. Imaging Graph., 78 (2019), 101657.
- [34] Shishir Maheshwari; T. Sunil Kumar A Comparison of Local Descriptor-based Data Augmentation Techniques for Glaucoma Detection using Retinal Fundus Images 2022 E-Health and Bioengineering Conference (EHB) Year: 2022 | Conference Paper | Publisher: IEEE
- [35] Siddhartha Mallick; Jayanta Paul; Nandita Sengupta; Jaya Sil Study of Different Transformer based Networks For Glaucoma Detection TENCON 2022 - 2022 IEEE Region 10 Conference (TENCON)Year: 2022
- [36] Sudeshna Pattanaik; Subhasikta Behera; Pratyusa Kumar Dwibedy; Santosh Kumar Majhi; Rosy PradhanAdaRes: ResNet50 with AdaSwarm for Glaucoma Classification & Detection 2022 3rd International Conference for Emerging Technology (INCET) Year: 2022 | Conference Paper | Publisher: **IEEE**
- [37] T. Khalil, M. U. Akram, S. Khalid, S. H. Dar, N. Ali, A study to identify limitations of existing automated systems to detect glaucoma at initial and curable stage, Int. J. Imaging Syst. Technol., 8 (2021).
- [38] Teresa Araújo; Guilherme Aresta; HrvojeBogunović Deep Dirichlet Uncertainty for Unsupervised Out-of-Distribution Detection of Eye Fundus Photographs in Glaucoma Screening 2022 IEEE International Symposium on Biomedical Imaging Challenges (ISBIC) Year: 2022 | Conference Paper | Publisher: **IEEE**
- [39] U. R. Acharya, S. Bhat, J. E. Koh, S. V. Bhandary, H. Adeli, A novel algorithm to detect glaucoma risk using texton and local configuration pattern features extracted from fundus images, Comput. Biol. Med., 88 (2017), 72-83.
- [40] V; Naganikhitha. M; Sai Meghana. U; Tirumala Tejaswi. V; Meghana. CH; Divya. Glaucoma Detection using Convolution Neural Networks Pavani. Y2023 7th International Conference on Computing Methodologies and Communication (ICCMC) Year: 2023 | Conference Paper | Publisher: **IEEE**
- [41] Y. Mlouhi; S. Souli; I. Jabri; T. Battikh An expert system for early glaucoma pathology detection A. Soltani; 2022 8th International Conference on Control, Decision and Information Technologies (CoDIT) Year: 2022
- [42] Yves Attry Kalin; Yash Bhardwaj; Subhash Arun Dwivedi; Arun Agrawal; Shravyam Risariya; Vivek Jha Analogizing the Potency of Deep Learning Models for Glaucoma Detection 2022 12th International Conference on

Cloud Computing, Data Science & Engineering (Confluence)